Kinetic Modeling of Slurry Propylene Polymerization using *rac*-Et(Ind)$_2$ZrCl$_2$/MAO

Ramon A. Gonzalez-Ruiz, Bernabe Quevedo-Sanchez, Robert L. Laurence, and Michael A. Henson
Dept. of Chemical Engineering, University of Massachusetts, Amherst, MA 01003

E. Bryan Coughlin
Dept. of Polymer Science and Engineering, University of Massachusetts, Amherst, MA 01003

DOI 10.1002/aic.10758
Published online January 24, 2006 in Wiley InterScience (www.interscience.wiley.com).

The slurry homopolymerization of propylene catalyzed by the isospecific metallocene rac-Et(Ind)$_2$ZrCl$_2$/MAO was investigated using a semi-batch reactor. A full factorial design with three temperatures (50, 65 and 75°C) and four monomer partial pressures (1.5, 2.5, 3.2, and 3.8 atm) was performed. Analysis by ^{1}H NMR revealed the formation of vinylidene, cis-2-butenyl and 4-butenyl end-groups. A kinetic model based on a coordination-insertion mechanism was developed to predict instantaneous reaction rate, molecular weights and polymer chain ends. The kinetic rate constants were estimated using a systematic optimization strategy. The model predicts that the insertion of the first propylene molecule is rate limiting with respect to propagation. Molecular weight decreases with temperature due to the high activation energy of the main chain transfer reaction (101 kJ/mol) relative to propagation (52 kJ/mol). The percentage of butenyl end-groups with respect to vinylidene decreases with temperature, thus predicting a lower activation energy for the β-hydride elimination after secondary insertion (27 kJ/mol).
 AIChE J, 52: 1824–1835, 2006
Keywords: Kinetic modeling, parameter estimation, olefin polymerization, metallocene catalyst, end-group analysis.

Introduction

The development of metallocene-based catalyst technology represents one of the most important innovations in the production of polyolefins. The benefit of metallocene catalysts is that they allow the production of tailored macromolecules, leading to new products such as syndiotactic polypropylene or syndiotactic polystyrene. Understanding process conditions and having control over them are also critical in the production of tailored macromolecules. Mathematical modeling of the polymerization process is a key step towards developing such understanding and affords opportunities for optimization.

Thermoplastic industries for polypropylene (PP) are mainly based on Ziegler-Natta catalyst technology. In 2000, the global demand for polyolefins was approximately 79 million metric tons, with polypropylene being nearly one-third of total consumption. Metallocene-catalyzed polypropylene accounted for less than 0.5% of this market. Nevertheless projections forecast substantial growth for metallocene-based polypropylene demand, which is expected to reach 20% of the total global propylene consumption by 2010.[1] Given these promising trends, efforts in academic and industrial laboratories are focused towards developing a better understanding of metallocene-catalyzed polyolefin processes for a variety of purposes, including future reactor design. Thus detailed knowledge of polymerization kinetics using metallocene catalysts is critical. Semi-batch or continuous laboratory-scale reaction systems are frequently used to determine kinetics parameters and to evaluate new reaction models.[2, 3]

Olefin polymerization kinetics have been investigated for a

Correspondence concerning this article should be addressed to E. B. Coughlin at coughlin@mail.pse.umass.edu and M. A. Henson at henson@ecs.umass.edu.
R.A. Gonzalez-Ruiz and B. Quevedo-Sanchez both contributed equally to this work.

wide variety of homogeneous metallocene catalyst systems.[4] Many experimental studies focused on identifying the individual steps of the kinetic mechanism.[5-10] However, only a few kinetic models have been validated using instantaneous reaction rate and molecular weight data. In some studies there was no attempt to even predict the molecular weight distribution (MWD) of the final polymer.[11-13] Some kinetic models are based on the assumption that chain initiation is instantaneous with respect to propagation.[14-16] In more recent models, the activation period was characterized by the non-instantaneous insertion of the first monomer molecule into the alkylated catalyst.[11-13, 17] Most researchers agree that metallocene catalysts systems have only one type of active center, which is supported by the fact that the molecular weight distribution of the final polymer typically follows a Schulz-Flory distribution. However Vela Estrada and Hamielec[15] proposed that a two-site model was required to fit their bimodal distributions for the molecular weight of polyethylene.

A common feature in several kinetic models is the inclusion of reversible reactions from which polymer chains with latent sites are produced from growing chains. Wester *et al*.[11] included the reversible formation of latent sites, which are considered to be misinserted chains or non-active Zr/MAO complexes that do not undergo further propagation. An equilibrium reaction between an active center and its latent dimerized product is included in some models[13, 16] to describe the second-order deactivation observed in the activity curve. This equilibrium reaction was proposed by Fisher *et al*.[14] when studying the Cp_2ZrCl_2/MAO system. Although uncommon, Ochoteco *et al*.[13] also included an irreversible bimolecular deactivation of the catalyst species to explain decreasing catalyst activity with increasing catalyst-cocatalyst premixing time.

A kinetic model capable of predicting reaction rate and MWD for the slurry polymerization of propylene using the catalyst system *rac*-Et(Ind)$_2$ZrCl$_2$/MAO was reported by Belleli *et al*.[17] Based on a polymeric multigrain model, they considered the existence of two types of active sites with different induction, formation and deactivation kinetics. Due to the complexity of the kinetic model, they had to assume values for ten parameters and to adjust nine parameters to match predicted and experimental productivities and average molecular weights. A propagation rate constant at 40°C of 365 L/(mol s) for the first site and 362 L/(mol s) for the second site was reported. Nele *et al*. developed a two-state kinetic model to describe the propylene polymerization behavior of fluxional metallocene catalysts,[18] and they also applied the model to *ansa*-metallocene catalysts.[19] The model can predict isotacticity, molecular weight and polymer crystallinity. However, we are not aware of any kinetic model in the literature that allows the prediction of instantaneous reaction rate, molecular weights and polymer end-groups resulting from competing chain transfer mechanisms.

Estimation of the kinetic parameters from experimental data is necessary to achieve qualitative predictions. Kinetic rate constants for initiation, propagation and termination reactions are usually estimated from polymerization rate data.[15, 17] By contrast, chain transfer reactions have no impact on the polymerization rate, but they strongly affect the molecular weight distribution. Therefore, the parameter estimation problem involves both on-line measurements of the reaction rate and end-of-batch measurements of molecular weight. Due to the complexity of the problem, estimates of kinetic parameters have been usually generated by trial-and-error procedures[15] or by invoking questionable approximations, such as using the time averaged value of the reaction rate.[16] Some papers contain very little information about the parameter estimation strategy,[11, 12] which is of paramount importance to obtain meaningful values of the kinetic rate constants.[17]

We present a kinetic investigation of slurry propylene polymerization with *rac*-Et(Ind)$_2$ZrCl$_2$/MAO (*rac*-ethylenebis (indenyl) zirconium dichloride / methylaluminoxane). The objectives of the work were to: (1) study the effects of monomer concentration and polymerization temperature on the polymerization behavior; (2) develop a kinetic model able to predict the instantaneous reaction rate, the molecular weight distribution and the percentage of unsaturated end-groups of the final polymer; and (3) estimate kinetic parameters by applying a systematic optimization technique using both on-line measurements of the reaction rate and end-of-batch measurements of the MWD and end-groups. This study represents the first step towards our long-term goal of developing a general and chemically based kinetic model that is applicable to many metallocene catalyst systems for polyolefin production.

Experimental

Materials

The metallocene complex *rac*-Et(Ind)$_2$ZrCl$_2$ and triisobutylaluminum (TIBA) 1.0 M solution in toluene were purchased from Sigma-Aldrich. Methylaluminoxane (MAO) 30% wt solution in toluene was donated by Albemarle Corp. (Baton Rouge, LA). The metallocene complex, MAO and TIBA were used without further purification. Propylene (grade 2.0, 99.9% pure) was supplied by BOC Gases (Murray Hill, NJ). Nitrogen (pre-purified grade) was supplied by Merriam Graves Corp. (Greenfield, MA). 3 Å molecular sieves from Sigma-Aldrich (St Louis, MO), Selexsorb COS (Alcoa World Chemicals, Houston, TX) and non-activated cuprous oxide (Engelhard Co., Iselin, NY) were used as adsorbents to purify the propylene.

Reactor

The semi-batch reactor is an Autoclave Engineers 500 mL ZipperClave®. Two gas monomer streams can be fed simultaneously to the reactor. Mass flows were measured by two Sierra Instruments SideTrak 840 Series mass flow controllers (0-5000 cm^3/min of air at 70°F and 1 atm). A purification train of adsorption beds ensured oxygen, moisture and CO removal from the monomer gas lines. The adsorbents for these beds were activated cuprous oxide for the oxygen trap and a combination of 3 Å molecular sieves and Selexsorb COS to remove water and carbon dioxide, respectively. A suitable gas supply line was built to safely provide the system with a reliable monomer flow. Check valves were installed upstream of the mass-flow controllers to avoid contamination from other gases and backflow. Excess flow valves were set in the monomer lines to prevent an uncontrolled gas leak should a line break or an accidental valve opening occur. The gas supply line is shown in Figure 1.

Pressure in the reactor was controlled by cascading an internal pressure controller to both mass flow controllers. As a safety measure, a F-type rupture disk (Oseco, burst pressure

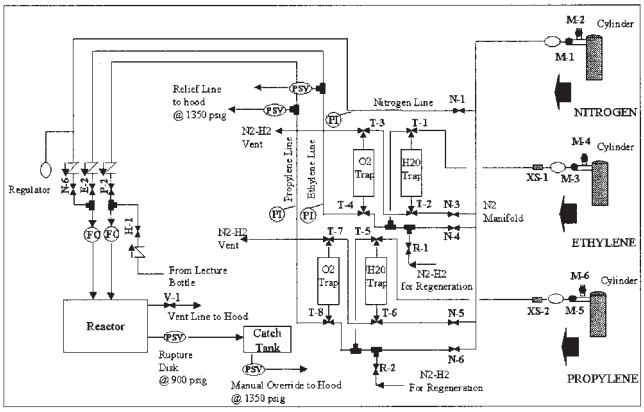

Figure 1. Gas supply line.

876 psig) was mounted at the top of the reactor. A Julabo FP50 MV Heating/Cooling System, using Thermal H5S bath fluid as heat transfer medium, allowed reactor temperature control from -20°C to 120°C. Mixing in the reactor was provided by a magnetically driven 45° pitched 4-blade turbine with a maximum speed of 3,000 rpm. Reactor temperature, pressure, gas flow and agitator speed were automatically controlled using a National Instruments LabView® software Virtual Instrument, interfaced to a Koyo Model 250 Programmable Logic Controller with a 205 Model CPU to handle all analog/digital inputs and outputs. A simplified scheme of the control system and equipment layout is presented in Figure 2.

Polymerization procedure

All polymerization runs were preceded by a system cleanup protocol to ensure the absence of moisture and oxygen in the reactor. A day before the experimental run, the vessel was heated to 80°C while a makeup stream of pre-purified nitrogen (2,500 cm^3/min of N_2 measured at 21°C at 1 atm) was purged through the reactor for 2 hours. The reactor was subsequently evacuated two times for 5 minutes and fresh nitrogen was used to refill the system. The system was cooled to room temperature under nitrogen flush and was then subjected to a positive static pressure test overnight. If the pressure test was satisfactory, the reactor was then heated to the desired polymerization temperature and loaded with 200 mL of toluene and 0.6 mL of 1.0 M triisobutyl aluminum (TIBA), which acted as a scavenger, via a stainless steel cylinder. Agitation was set at the desired speed, and the vessel was saturated with monomer at the experimental partial pressure. The reaction began with the injection of a previously activated catalyst/cocatalyst mixture using inert gas overpressure. We found that the activated catalyst was very sensitive to oxygen and water impurities. Therefore, the precursor was prepared in dry boxes with oxygen levels less than 20 ppm and water levels of less than 10 ppm using 18-mL commercial vials. Typically, 2.8 μmol of catalyst in toluene solution of 6×10^{-4} mol/L were mixed with the MAO solution without stirring for 30 minutes. Vapor-liquid equilibrium between propylene and toluene was estimated using the Peng-Robinson equation for both phases to calculate the concentration of propylene in the liquid phase.[20] Polymerizations were finished by stopping the monomer gas flow injecting 10 mL of methanol and degassing the reactor. The reactor contents were washed overnight with a methanol/hydrochloric acid mixture and dried under vacuum.

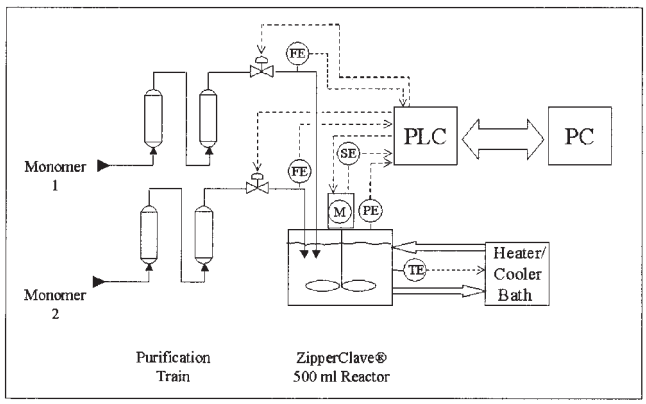

Figure 2. Semi-batch reaction system.

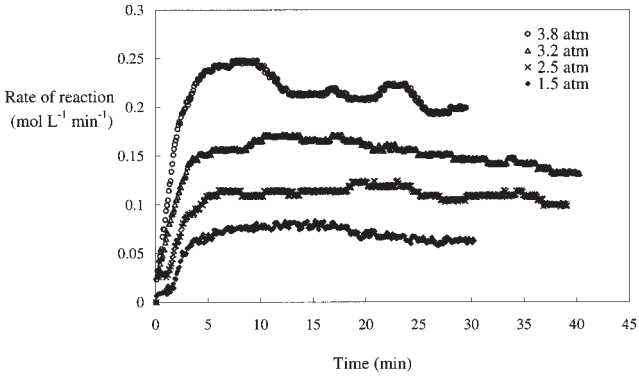

Figure 3. Reaction rate profiles at 65°C for four different partial pressures of propylene: (○) 3.8 atm, (Δ) 3.2 atm, (×) 2.5 atm, (◆) 1.5 atm.

Characterization methods

The molecular weight distributions of the polypropylenes were measured by Gel Permeation Chromatography on a Polymer Laboratories PL-220 high temperature GPC with a Differential Refractive Index Detector (wavelength 633 nm). 1,2,4-tricholobenzene was used as solvent at 135°C. Absolute measurements of molecular weights were calculated using a universal calibration method against narrow polystyrene standards. Mark-Houwink constants for polystyrene, K = 0.0172 and α = 0.67, and isotactic polypropylene (iPP), K = 0.0137 and α = 0.75, were used.[21] Polymer end-groups were analyzed by high temperature ^{1}H NMR spectroscopy, using a Bruker AVANCE 400 NMR spectrometer at 100°C and 1,1,2,2-tetrachloroethane-d_2 as solvent. Instrument conditions were as follows: pulse angle, 30°; pulse repetition, 5.0 s; spectral width, 8278 Hz; number of scans, 500.

Results and Discussion

Kinetics of polymerization

A full factorial experimental design with four propylene partial pressures (1.5, 2.5, 3.2 and 3.8 atm) and three levels of temperature (50, 65 and 75°C) was performed in the semi-batch reactor. The temperature range was selected based on the

conditions of commercial polypropylene processes, such as the Spheripol process, which range between 60 and 80°C.[22] Polymerization rate curves (Figures 3 and 4) were consistent with previous profiles shown in the literature for metallocene systems in semi-batch reactors.[5, 11, 13, 17, 23] As reported by other authors,[24] there was an induction period of about 1-2 min after catalyst injection during which the pressure did not drop sufficiently to require monomer flow to maintain the internal pressure set point. Time zero was established when propylene gas began flowing into the reactor. Polymerization rate profiles were characterized by an activation period before a maximum rate was reached, followed by deactivation decay with time. For runs performed at the same temperature (Figure 3), the reaction rate increased with the partial pressure of propylene due to the higher concentration of monomer in the liquid phase.[9] For runs performed at the same propylene partial pressure (Figure 4), temperature accelerated the reaction rate. The deactivation decay was more significant at high temperatures and pressures, giving a more pronounced maximum rate of reaction. Experimental measurements of activity of the polymerization, expressed as kg PP/(molZr M h), appeared to be insensitive to monomer concentration while they increased with polymerization temperature (Table 1).

Monomer concentration and temperature effect on molecular weight

The MWD of the final polymer is determined by the rate of chain transfer reactions relative to the propagation rate. For a single-center catalyst, molecular weight of the produced polymer follows a Schultz-Flory distribution with a polydispersity (M_w/M_n) equal to 2. Polydispersities measured for our polypropylene ranged from 2.01 to 2.39 (Table 2). The deviation from the theoretical value of two can be explained by variation of propylene concentration in the liquid phase.[18] Therefore, we assumed that our metallocene system was acting as a single-center catalyst. Both number average and weight average molecular weight decreased with increasing polymerization temperature (Table 2). This result shows that temperature accelerates the rate of chain transfer reactions with respect to propagation. In other words, the activation energy of the main chain transfer reaction is higher than the activation energy of propagation.[16]

The effect of monomer concentration on molecular weight is

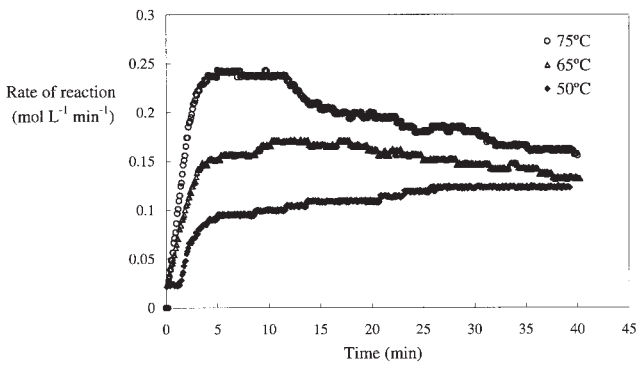

Figure 4. Reaction rate profiles at 3.2 atm of partial pressure of propylene for three different temperatures: (○) 75°C, (Δ) 65°C, (×) 50°C.

Table 1. Catalyst Activity for Experimental Runs

Run[(a)]	*T* °C	P atm	M mol/L	Time min	Activity[(b)] kg PP/ (mol Zr [M] h)
1	50	1.5	0.60	55	15600
2	50	2.5	1.09	40	9900
3	50	3.2	1.47	40	10600
4	50	3.8	1.83	30	10300
5	65	1.5	0.42	30	24100
6	65	2.5	0.78	40	20500
7	65	3.2	1.05	40	20000
8	65	3.8	1.30	30	21400
9	75	1.5	0.33	30	35100
10	75	2.5	0.63	40	25900
11	75	3.2	0.85	40	30800
12	75	3.8	1.05	20	36600

[(a)]Polymerization conditions: 200 mL toluene, $[Zr]_0 = 1.4\ 10^{-5}$ mol/L, MAO/Zr = 3000, agitation speed 1250 rpm. [(b)]Best activity for each polymerization condition.

important to elucidate whether the main chain transfer reaction is bimolecular (monomer dependent) or unimolecular.[6, 9] A bimolecular chain transfer to the monomer gives a constant molecular weight with respect to monomer concentration, while unimolecular chain transfer to the metal gives a linear increase in molecular weight with monomer concentration.[25] Results from Resconi *et al.*[6] for $Et(Ind)_2ZrCl_2$/MAO in liquid propylene at 50°C showed that M_w increased for a monomer concentration range from 0 to 10 mol/L. This trend can be separated into two regimes: a linear increase in M_w from 0 to 1 mol/L and a slower increase from 1 to 10 mol/L. According to our results (Table 2), M_w appeared to be constant with increasing monomer concentration at 65 and 75°C within the studied monomer concentration range. For the runs performed at 50°C, M_w showed a large increase for a monomer concentration range between 0.6-1.09 mol/L, followed by a slight decrease at concentrations from 1.09 to 1.83 mol/L. Therefore, our experimental results appeared to be consistent with the assumption that the main chain transfer reaction was bimolecular giving a constant M_w with respect to monomer concentration.

End-group analysis of the polymer

Analysis of end-group configurations of the polypropylene chain is the technique used to determine the chain transfer reactions taking place during the polymerization. For *rac*-$Et(Ind)_2ZrCl_2$/MAO, the vinylidene end-group (Figure 5) formed by β-hydride elimination has been reported as the dominant termination.[10, 26] The olefin region of the ^1H NMR spectra (400 MHz, TCE-d_2, 100°C) of the PP samples polymerized at a monomer concentration of approximately 1 mol/L are shown in Figure 6*. PP samples from *rac*-$Et(Ind)_2ZrCl_2$/MAO showed four olefinic end-groups: vinylidene (structure **a** in Figure 5, 4.68 H^{1A} singlet, 4.75 H^{1B} singlet) formed by β-hydride elimination; *cis*-2-butenyl (structure **b**, 5.39-5.54 H^2 and H^3, complex multiplet) produced by β-hydride elimination after a secondary insertion; allyl (structure **c**, 4.94-5.05 H^{5A} and H^{5B}, 5.75-5.95 H^6 complex multiplet) formed by β-methyl elimination; and a triplet at 5.20 ppm, which has been assigned

*The spectra of the PP samples obtained at different reaction conditions are available as supplementary information.

Table 2. MWD and End-Groups Characterization for Experimental Runs

			MWD[a]			% Unsaturated Groups				
Run	T °C	P atm	M_n g/mol	M_w g/mol	M_w/M_n	**a** Vinylidene	**b** 2-Butenyl	**c** 4-Butenyl	**d** Allyl[b]	**e** Internal Vinyl
1	50	1.5	7580	18100	2.39	41.1	30.2	18.4	n.d	10.3
2	50	2.5	15700	31700	2.01	32.1	40.8	16.3	n.d	10.8
3	50	3.2	12800	29700	2.32	37.4	31.7	14.1	n.d	16.8
4	50	3.8	12800	26600	2.09	37.4	40.5	11.0	n.d	11.1
5	65	1.5	6210	13900	2.24	65.3	17.0	11.8	n.d	5.9
6	65	2.5	8120	17700	2.18	51.2	26.3	13.5	n.d	9.0
7	65	3.2	6870	15000	2.19	46.5	26.5	14.4	n.d	12.7
8	65	3.8	9170	19000	2.07	37.2	32.0	21.6	n.d	9.2
9	75	1.5	4340	8900	2.06	70.6	2.6	3.7	7.8	15.3
10	75	2.5	5590	12100	2.16	65.3	9.9	8.9	6.4	9.4
11	75	3.2	7330	17000	2.31	60.3	15.8	6.9	n.d	16.9
12	75	3.8	5640	12300	2.19	57.1	12.0	8.8	10.2	11.8

[a]Measured using GPC with two injections per sample. [b]n.d: peak not detected.

to the vinylic proton in 4-butenyl (structure **d**, 5.20 H^4 triplet).[7,8,26] The unsaturated group 4-butenyl was only detected when the 2-butenyl end-group was present. We hypothesize that the formation of 4-butenyl is associated with that of 2-butenyl. However, 4-butenyl production due to isomerization of 2-butenyl during polymer work-up or NMR analysis can be ruled out, since Carvill *et al.*[7] reported that 2-butenyl group did not isomerize to the 4-butenyl end-group after 48 h at 103°C. Also, Resconi *et al.*[8, 26] proved that the *cis*-2-butenyl group was stable in the presence of added acids (*p*-toluene-sulfonic-acid, $C_2D_2Cl_4$, 130°C, 30 minutes). With these experimental evidences, we postulate that the 4-butenyl end-group is formed in an isomerization reaction catalyzed by a zirconocene hydride complex during polymerization. Further experiments to confirm this hypothesis are underway.

Another important feature of the unsaturated end-groups was that the two vinylidene peaks were unequal in intensity. This is due to the presence of a symmetrical vinylidene overlapping the lowest field vinylidene peak (structure **e**).[8, 26-28] The internal vinylidene has been postulated to result from a propylene insertion into an allylic activated zirconocene cation. This mechanism involves the reversible formation of a zirconocene (allyl) dihydrogen complex.[27, 29] Note that the internal vinylidene is not an end-group, but rather an internal unsaturation.

The amount and nature of the chain end-groups is influenced not only by the catalyst structure, but also by process conditions.[7] This fact is corroborated by the percentages of unsaturated end-groups from the polymer obtained in each experimental run (Table 2). Vinylidene and 2-butenyl were the dominant end-groups for the studied conditions. The percentage of 2-butenyl decreased with increasing temperature, indicating that temperature enhances formation of vinylidenes with respect to 2-butenyl unsaturations. The trend with pressure was not clear, since the percentage of 2-butenyl remained constant with monomer concentration at 75°C, but appeared to have a slight increase with monomer pressure at 65 and 50°C. Allyl end-groups were detected only in polymer chains produced at 75°C, indicating that β-methyl chain transfer reaction has a larger activation energy than β-hydride elimination.

A question that arises is if the vinylidene end-groups were produced by bimolecular β-hydride transfer to the monomer or by unimolecular β-hydride transfer to the metal. These two chain transfer reactions cannot be distinguished by NMR analysis since both produce the same end-groups. Instead, the dependency of molecular weight on monomer concentration must be investigated.[6, 9, 25] As discussed previously, our experimental results do not show a clear dependency, and therefore

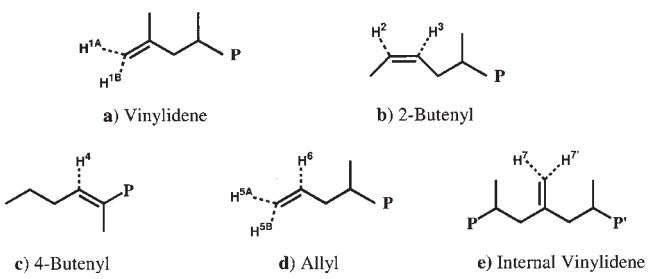

Figure 5. Proton numbering of unsaturated end-groups and internal vinylidene.

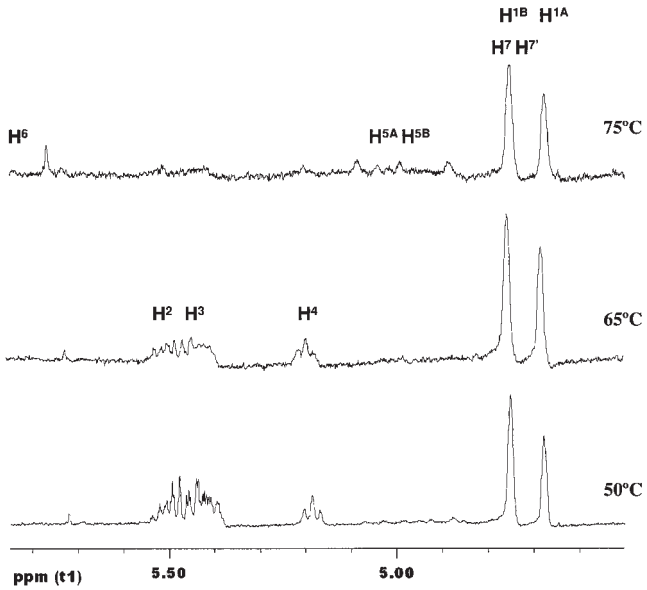

Figure 6. ^{1}H NMR olefinic region (400 MHz, 1,1,2,2-tetrachloroethane-d_2, 100°C, Ref. C_2HDCl_4 at 5.95 ppm) of iPP from *rac*-Et(Ind)$_2$ZrCl$_2$/MAO polymerized at approximately M = 1 mol/L and temperatures 50, 65 and 75°C (runs 2, 7 and 12 in Table 1).

Table 3. Kinetic Model for Metallocene Catalyzed Polymerization of Propylene

Kinetic Model	
Initiation	$C^* + M \xrightarrow{k_{in}} R_1$
Propagation	$R_i + M \xrightarrow{k_p} R_{i+1}$
Chain transfer to monomer	$R_i + M \xrightarrow{k_{tr}} D_i + R_1$
Deactivation	$R_i \xrightarrow{k_d} D_i + C_d^*$
Secondary insertion	$R_i + M \xrightarrow{k_s} P_{i+1}$
Propagation after mis-insertion	$P_i + M \xrightarrow{k_{sp}} R_{i+1}$
Chain transfer after mis-insertion	$P_i + M \xrightarrow{k_{str}} D_i + R_1$

Species			
C^*	catalyst activated complex	D_i	dead chain with "i" monomer units
M	monomer	P_i	chain with "i" monomer units with misinsertion
R_i	active chain with "i" monomer units	C_d^*	inactive catalyst complex

we assumed that M_w is independent of monomer concentration. This assumption implies that the vinylidene end-groups were produced by β-hydride transfer to the monomer.

Kinetic Model

A chemically based kinetic model was developed from the available experimental data. The kinetic mechanism shown in Table 3 is based on the following assumptions: (i) the activated complex acts as a single-center catalyst; (ii) chain growth is initiated by the noninstantaneous insertion of the first monomer molecule; (iii) chain transfer following a primary (1,2) insertion occurs by bimolecular β-hydride transfer to the monomer, producing a vinylidene-terminated dead chain and liberating an active center; (iv) unimolecular deactivation of growing chains produces deactivated catalyst, which no longer undergoes propagation; (v) β-methyl elimination is not included due to its low frequency relative to β-hydride elimination under the studied conditions and; (vi) a secondary (2,1) insertion produces a mis-inserted chain, which can undergo propagation or β-hydride transfer to the monomer to produce a butenyl-terminated chain. We postulate that 4-butenyl end-groups are formed in an isomerization reaction from *cis*-2-butenyl during polymerization, thus both unsaturations are considered as butenyl end-groups. The occurrence of two consecutive secondary insertions is not included due to its low probability.

The reactor volume change attributable to polypropylene accumulation in the liquid phase is neglected due to the small polypropylene production rates achieved. Therefore, the material balance on monomer in the semi-batch reactor is given by

$$\frac{dM}{dt} = \frac{F}{V} - k_{in}MC^* - (k_p + k_{tr} + k_s)ML_0 - (k_{sp} + k_{str})MQ_0 \quad (1)$$

where F is the propylene molar flow, and $L_0 = \sum_{i=1}^{\infty} R_i$ and $Q_0 = \sum_{i=2}^{\infty} P_i$ are the concentration of active and mis-inserted chains of all lengths, respectively. The consumption of monomer in the initiation, secondary insertion and chain transfer reactions is considered negligible compared to the consumption of monomer by propagation (the long chain approximation). Since the pressure is held constant during the polymerization, the concentration of propylene in the reaction mixture is approximately constant with time ($dM/dt \approx 0$). Therefore, the propylene flow provides a direct measurement of the rate of reaction as follows:

$$\frac{F}{V} = k_p ML_0 \quad (2)$$

Material balances for active chains, mis-inserted chains, dead chains and catalyst activated complex are written below where $k' = kM$:

$$\frac{dR_1}{dt} = k'_{in}C^* - k'_pR_1 - k'_{tr}(R_1 - L_0) - k_dR_1 - k'_sR_1 + k'_{str}Q_0 \quad (3)$$

$$\frac{dR_2}{dt} = k'_p(R_1 - R_2) - k'_{tr}R_2 - k_dR_2 - k'_sR_2 \quad (4)$$

$$\frac{dR_i}{dt} = k'_p(R_{i-1} - R_i) - k'_{tr}R_i - k_dR_i - k'_sR_i + k'_{sp}P_{i-1} \quad \text{for } i > 2 \quad (5)$$

$$\frac{dP_i}{dt} = k'_sR_{i-1} - k'_{sp}P_i - k'_{str}P_i \quad \text{for } i > 1 \quad (6)$$

$$\frac{dD_1}{dt} = k'_{tr}R_i + k_dR_i \quad (7)$$

$$\frac{dD_i}{dt} = k'_{tr}R_i + k_dR_i + k'_{str}P_i \quad \text{for } i > 1 \quad (8)$$

$$\frac{dC^*}{dt} = -k'_{in}C^* \quad (9)$$

The method of moments is used to characterize the molecular weight distribution (MWD) of the polymer chains, where L_n,Q_n and U_n are the n-th order moments for the distribution of active, mis-inserted and dead chains, respectively:

$$L_n = \sum_{i=1}^{\infty} i^n R_i; \quad Q_n = \sum_{i=2}^{\infty} i^n P_i; \quad U_n = \sum_{i=1}^{\infty} i^n D_i \quad (10)$$

Ordinary differential equations (ODEs) for the zeroth-, first- and second-order moments of the distribution of polymer chains are obtained by multiplying Eqs. 3 to 8 by i^0, i^1 and i^2, and then summing over all values of i as in Eq. 10. The zeroth moment for dead chains is divided in vinylidene-terminated chains $(U_0)_V$ and butenyl-terminated chains $(U_0)_B$ to predict the percentage of each end-group with respect to the total number of unsaturations. The resulting equations are:

$$\frac{dL_0}{dt} = k'_{in}C^* - (k_d + k'_s)L_0 + (k'_{sp} + k'_{str})Q_0 \tag{11}$$

$$\frac{dL_1}{dt} = k'_{in}C^* + k'_pL_0 - (k_d + k'_s)L_1 + k'_{tr}(L_0 - L_1) + k'_{sp}(Q_0 + Q_1) + k'_{str}Q_0 \tag{12}$$

$$\frac{dL_2}{dt} = k'_{in}C^* + k'_p(L_0 + 2L_1) - (k_d + k'_s)L_2 + k'_{tr}(L_0 - L_2) + k'_{sp}(Q_0 + 2Q_1 + Q_2) + k'_{str}Q_0 \tag{13}$$

$$\frac{dQ_0}{dt} = k'_sL_0 - (k'_{sp} + k'_{str})Q_0 \tag{14}$$

$$\frac{dQ_1}{dt} = k'_s(L_0 + L_1) - (k'_{sp} + k'_{str})Q_1 \tag{15}$$

$$\frac{dQ_2}{dt} = k'_s(L_0 + 2L_1 + L_2) - (k'_{sp} + k'_{str})Q_2 \tag{16}$$

$$\frac{d(U_0)_V}{dt} = (k_d + k'_{tr})L_0 \tag{17}$$

$$\frac{d(U_0)_B}{dt} = k'_{str}Q_0 \tag{18}$$

$$\frac{dU_1}{dt} = (k_d + k'_{tr})L_1 + k'_{str}Q_1 \tag{19}$$

$$\frac{dU_2}{dt} = (k_d + k'_{tr})L_2 + k'_{str}Q_2 \tag{20}$$

An analytical solution for $L_0(t)$ is obtained by solving Eqs. 9, 11 and 14 with the appropriate M value shown in Table 1, and the initial conditions $C^*(0) = C_0^*$ and $L_0(0) = Q_0(0) = 0$, where C_0^* is the initial concentration of activated complex. Then an analytical expression for the reaction rate is derived from Eq. 2. It was found that a reasonable simplifying assumption is to consider that the rate of secondary insertion, propagation of the mis-inserted chain and chain transfer after a secondary insertion do not affect the rate of reaction. The reaction rate for this simplified model comprised of initiation, propagation, chain transfer to monomer and deactivation has the following form:

$$r(t) = k_pML_0 = \frac{k_pC_0^*k_{in}M^2}{k_d - k_{in}M}\left[e^{-k_{in}Mt} - e^{-k_dt}\right] \tag{21}$$

This expression for the reaction rate is in agreement with previous modeling work for metallocene systems.[15] The polymerization rate does not depend on the rate constant of the chain transfer to monomer reaction, which will have a large effect on the molecular weight.

The MWD of the final polymer is characterized by the number and weight average molecular weights:

$$M_n = m\,\frac{L_1 + Q_1 + U_1}{L_0 + Q_0 + U_0} \tag{22}$$

$$M_w = m\,\frac{L_2 + Q_2 + U_2}{L_1 + Q_1 + U_1} \tag{23}$$

where m is the molecular weight of propylene, and $U_0 = (U_0)_V + (U_0)_B$. The kinetic model predicts the formation of vinylidene-terminated chains and butenyl-terminated chains. The percentage of butenyl end-groups (B) relative to the total number of unsaturations is given by:

$$B = 100 \times \frac{(U_0)_B}{(U_0)_B + (U_0)_V} \tag{24}$$

Numerical solutions for M_n, M_w and B are obtained solving Eqs. 9 and 11 to 20 with the following initial conditions: $C^* = C_0^*$, $L_0 = L_1 = L_2 = 0$, $Q_0 = Q_1 = Q_2 = 0$, and $U_0 = U_1 = U_2 = 0$.

Parameter Estimation

The kinetic rate constants of the model were estimated from on-line measurements of the reaction rate and end-of-batch measurements of the molecular weight distribution and percentage of unsaturated end-groups. The kinetic rate constants were assumed to have an Arrhenius dependence with temperature:

$$k_i(T) = A_i\exp\left[-\frac{E_i}{T}\right] \tag{25}$$

where the activation energy E_i and the pre-exponential factor A_i for each rate constant k_i serve as adjustable parameters.

For simplicity, the kinetic rate constants for initiation, propagation and deactivation were assumed to only affect the rate of reaction, while the kinetic rate constants for chain transfer to monomer, secondary insertion, propagation after mis-insertion and chain transfer after mis-insertion were assumed to only affect the molecular weight and percentage of end-groups. This simplification allowed the estimation of kinetic parameters to be decomposed into two sequential subproblems.[17] First, k_{in}, k_p and k_d were estimated from polymerization rate data by solving the following least-squares problem:

Table 4. Kinetic Rate Constants Estimated from Rate of Reaction, MWD and End-Group Analysis Data

	k_{in} (L mol^{-1} s^{-1})	k_p (L mol^{-1} s^{-1})	k_d (s^{-1})	k_M (L mol^{-1} s^{-1})	k_s (L mol^{-1} s^{-1})	k_{sM}[(a)] (L mol^{-1} s^{-1})
ln A_i	10.24	24.05	13.42	35.55	8.50	>6
E_i (kJ/mol)	43.05	52.32	62.03	100.65	26.58	0
T (°C)						
50	3.07E−03	9.75E+01	6.36E−05	1.48E−01	2.50E−01	>4E+02
65	6.27E−03	2.31E+02	1.77E−04	7.78E−01	3.87E−01	>4E+02
75	9.74E−03	3.95E+02	3.34E−04	2.18E+00	5.08E−01	>4E+02

[(a)]Values greater than the reported one affect less than 1/1000 the absolute value of the objective function.

$$\min_{\theta_1} \sum_{i=1}^{N_i} \sum_{j=1}^{N_j} [p^i(t_j) - \hat{p}^i(t_j)]^2 \tag{26}$$

where $p^i(t_j)$ represents the measured polymerization rate at time t_j for experimental run i, the " " denotes a predicted value obtained from the kinetic model, N_j is the total number of data points for i-th semi-batch run, and N_i=12 is the total number of runs. The kinetic parameters $\theta_1 = \{A_{in}, E_{in}, A_p, E_p, A_d, E_d\}$ serve as decision variables in the first optimization problem. The difference between the experimental and predicted reaction rates was not scaled to emphasize runs with higher rates and more pronounced deactivation decay. We found that this scaling was important to generate good estimates of the initiation and deactivation rate constants. Second, the rate constants of the reactions that mainly affect molecular weight and percentage of end-groups were estimated from molecular weight data as well as the measured percentage of butenyl end-groups (B) by solving the following least-squares problem:

$$\min_{\theta_2} \sum_{i=1}^{N_i} \left(\left[\frac{M_n(t_f^i) - \hat{M}_n(t_f^i)}{M_n(t_f^i)} \right]^2 + \left[\frac{M_w(t_f^i) - \hat{M}_w(t_f^i)}{M_w(t_f^i)} \right]^2 + \left[\frac{B(t_f^i) - \hat{B}(t_f^i)}{B(t_f^i)} \right]^2 \right) \tag{27}$$

where t_f^i is the final time for the i-th experiment. The estimated parameters $\theta_2 = \{A_{tr}, E_{tr}, A_s, E_s, A_{sp}, E_{sp}, A_{str}, E_{str}\}$ serve as decision variables, with the first set of kinetic parameters (ϑ_1) fixed at their previously determined values since they primarily affect the polymerization rate. The optimization problem was solved by temporally discretizing the kinetic model equations using orthogonal collocation on finite elements.[30]

Because the second set of parameters (ϑ_2) has some effect on the rate of reaction and the first set of parameters (ϑ_1) affects the MWD, a one step optimization was performed by combining the objective functions (26) and (27) using weighting factors that roughly equalized the absolute value of the two objective functions. Parameter values obtained from solution of the sequential estimation problem were used as initial guesses for the one step optimization problem. The optimization problem was coded in AMPL, and the nonlinear solver program CONOPT was used to obtain kinetic parameters that minimized the combined objective function.

As shown by the simplified expression for the reaction rate (eq. 21), the initial concentration of activated complex C_0^* was needed to determine the kinetic parameters. The activated complex is a cationic species generated in an equilibrium reaction between the zirconocene molecule and MAO. In our experimental procedure, the catalyst/MAO mixture was premixed for 30 minutes prior to injection into the reactor to achieve an equilibrium concentration of activated complex that depends on the MAO/Zr ratio and temperature. Chien and Sugimoto[5] reported that for the *rac*-ethylenebis(4,5,6,7-tetrahydro-1-indenyl)zirconium dichloride/MAO species, approximately two-thirds of the metallocene becomes catalytically active at 30°C for MAO/Zr ratios greater than 3500. Several methods including chemical labeling[31] and quenched flow[32] have been proposed to determine the amount of active catalytic complex. We performed a quenched flow experiment by stopping the polymerization reaction with CH_3-OD at different reaction times. From this experiment, more than 63% of the original zirconocene was estimated to be active at 25°C. However the results from this experiment were not conclusive, and for the purpose of kinetic parameter estimation we assumed that 100% of the zirconocene molecules were activated in the equilibrium reaction with MAO.

A growing polypropylene chain with a last inserted 2,1 unit undergoes monomer insertion at a lower rate due to steric hindrance.[33] For the metallocene system studied in this paper, Busico *et al.*[25] reported k/k_{ps} for the hydro-oligomerization of propylene at 60°C by GC analysis. This result suggests that a high frequency of mis-insertions should yield a significant decrease in reaction rate. In our analysis, the effect of mis-inserted chain propagation on the reaction rate was dominated by the higher frequency of the competing chain transfer reactions that produce a butenyl-terminated chain. The inclusion of the propagation reaction for a mis-inserted chain did not improve the prediction of reaction rate, since k_{sp} appears in the model equations as a lumped parameter $k_{sp} + k_{str}$. Furthermore, the inclusion of the propagation reaction resulted in non-convergence of the optimization problem involving end-of-batch measurements (eq. 27). For these reasons the propagation of mis-inserted chains was neglected in the subsequent analysis.

The combined optimization problem produced a very large value of the chain transfer rate constant after secondary insertion (k_{str}), which did not affect the prediction of reaction rate and ensured that a chain with a mis-inserted monomer unit would produce a butenyl-terminated chain. Therefore, k_{str} was simply set equal to a sufficiently large value and removed from the optimization problem. Furthermore, the experimental percentage of butenyl end-groups for run 9 was not used for estimation because the peak intensities were close to the limit of detection.

When all these considerations are taken into account, solution of the combined optimization problem produced the kinetic parameter values reported in Table 4. Simulation results for the polymerization rate show that the model captured the

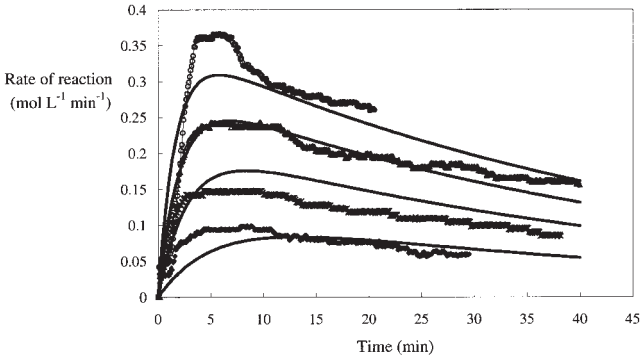

Figure 7. Measured polymerization rate (scattered points) and model prediction (solid line) at 75°C and four partial pressures of propylene: (○) 3.8 atm, (Δ) 3.2 atm, (×) 2.5 atm, (◆) 1.5 atm.

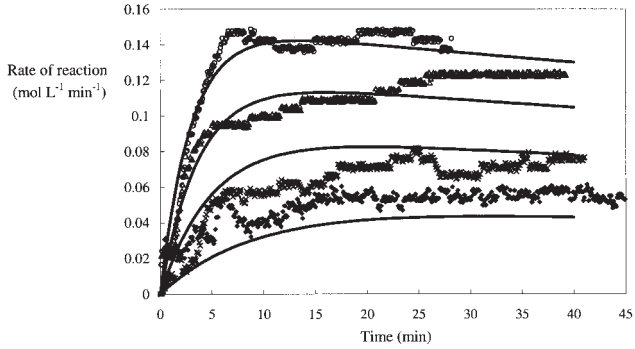

Figure 9. Measured polymerization rate (scattered points) and model prediction (solid line) at 50°C and four partial pressures of propylene: (○) 3.8 atm, (Δ) 3.2 atm, (×) 2.5 atm, (◆) 1.5 atm.

behavior of the experimental rate profiles (Figures 7-9) despite difficulties associated with impurities and slow temperature control. The model predicted an increasing reaction rate at high monomer concentrations and temperatures and also produced a steeper decay in the rate of reaction at higher propylene concentrations, thereby producing a more pronounced maximum in activity. A simple expression for the time at which the maximum reaction rate is achieved can be derived from Eq. 21:

$$t_{\max} = \frac{\ln\left(\frac{k_{in}M}{k_d}\right)}{k_{in}M - k_d} \tag{28}$$

The model predicts that the maximum polymerization rate is not function of k_p, and for the estimated parameters t_{max} decreases with increasing monomer concentration and reaction temperature. This result is in agreement with our experimental data (Figures 7-9). The small value of k_{in} relative to k_p in Table 4 supports the hypothesis that the insertion of the first monomer unit is rate limiting with respect to chain propagation.[12, 34] Therefore, the activation period is modeled by the non-instantaneous insertion of the first propylene molecule.[11, 13]

Predicted and measured values of M_n and M_w at the end of the batch are compared in Table 5, while the monomer concentration dependence of M_w is illustrated in Figure 10. The predicted polydispersity (M_w/M_n) is a constant equal to two since the kinetic model assumes that the activated complex acts as a single-center catalyst and predicts a theoretical Schultz-Flory distribution of molecular weights. Both M_n and M_w are predicted to be independent of monomer concentration because the chain transfer reactions are bimolecular and have the same monomer dependency as the propagation rate. However, the experimental trends are less clear and seem to deviate from the model predictions at the lowest temperature. The model predicts decreasing molecular weight with temperature, in agreement with our experimental data. This trend is explained by the high activation energy of the β-hydride elimination reaction after primary insertion (100.6 kJ/mol) relative to the activation energy of the propagation reaction (50.3 kJ/mol).

The predicted results for the production of butenyl-terminated chains relative to vinylidene-terminated chains (Table 6 and Figure 11) show a constant value with respect to monomer concentration. This trend appears to be consistent with experimental values at 50°C and 75°C but inconsistent with the trend at 65°C. As observed experimentally, the model predicts a decreasing percentage of butenyl-terminated chains with increasing temperature. This result is explained by the low activation energy of the mis-insertion reaction (26.6 kJ/mol) relative to the activation energy of the bimolecular β-hydride elimination reaction (100.6 kJ/mol). Another prediction generated by the kinetic model is the percentage of 2,1 insertions

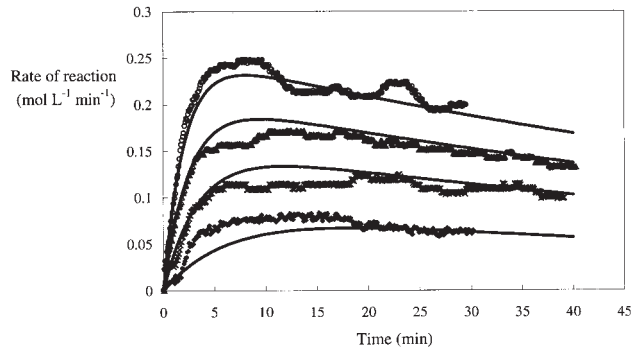

Figure 8. Measured polymerization rate (scattered points) and model prediction (solid line) at 65°C and four partial pressures of propylene: (○) 3.8 atm, (Δ) 3.2 atm, (×) 2.5 atm, (◆) 1.5 atm.

Table 5. Measured and Predicted Molecular Weights

	Experimental			Predicted		
Run	M_n g/mol	M_w g/mol	M_w/M_n	M_n g/mol	M_w g/mol	M_w/M_n
1	7580	18100	2.39	10366	20637	2.00
2	15700	31700	2.01	10378	20662	2.00
3	12800	29700	2.32	10382	20669	2.00
4	12800	26600	2.09	10383	20672	2.00
5	6210	13900	2.24	8393	16716	2.00
6	8120	17700	2.18	8398	16726	2.00
7	6870	15000	2.19	8399	16729	2.00
8	9170	19000	2.07	8400	16730	2.00
9	4340	8900	2.06	6230	12401	2.00
10	5590	12100	2.16	6232	12406	2.00
11	7330	17000	2.31	6233	12407	2.00
12	5640	12300	2.19	6233	12408	2.00

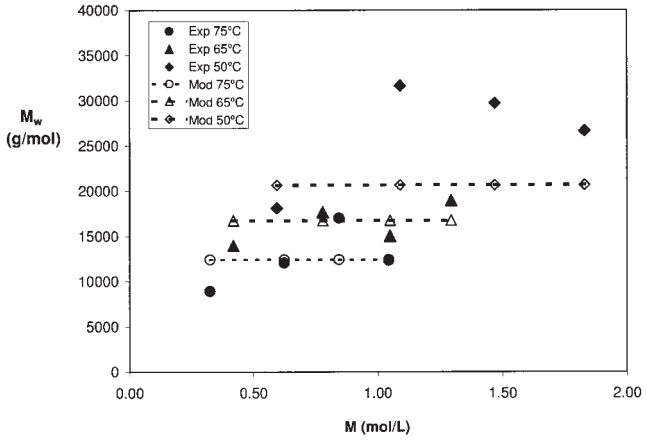

Figure 10. Measured weight average molecular weight (solid points) and model prediction (lines) *vs.* monomer concentration at 50°C (◆), 65°C (▲), and 75°C (●).

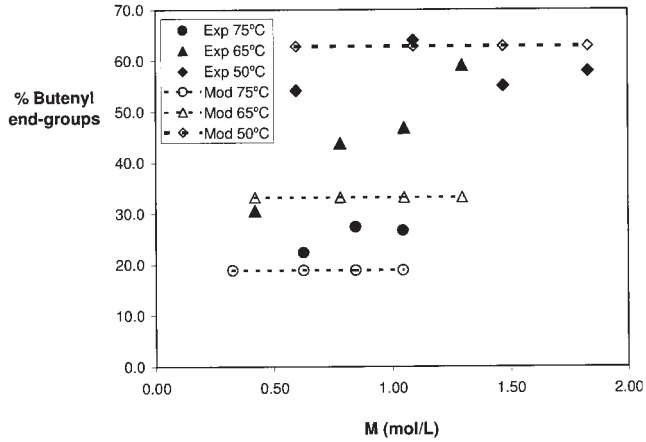

Figure 11. Measured percentage of butenyl end-groups (solid points) and model prediction (lines) *vs.* monomer concentration at 50°C (◆), 65°C (▲), and 75°C (●).

relative to regioregular 1,2 insertions ($k_s/(k_p + k_s)$). Table 7 shows that the percentage of regioirregular 2,1 insertions decreases with increasing temperature due to the lower activation energy of mis-insertion relative to propagation. This result is consistent with previous results reported in the literature for the studied catalyst system.[25] However, the trend is inconsistent with the small increasing degree of secondary insertion that Resconi *et al.*[26] reported for polymerization in liquid propylene using the studied catalyst.

Conclusions

A kinetic model for the semi-batch slurry polymerization of propylene with *rac*-Et(Ind)$_2$ZrCl$_2$/MAO as catalyst system has been developed. Polymerization temperatures from 50 to 75°C and propylene partial pressures from 1.5 to 3.8 atm were explored. The kinetic model was based on the key mechanistic steps of the coordination-insertion mechanism of single site metallocene olefin polymerization catalysts. Contrary to some kinetic models reported in the literature,[14-16] this work suggests that the activation period is due to the non-instantaneous insertion of the first monomer unit.[11-13, 17] The chain transfer reactions were delineated from a detailed ^{1}H NMR analysis of the unsaturated chain end-groups. The relative amount of each end-group depended on polymerization conditions. Allyl end-groups were only present at 75°C, while 2-butenyl and 4-butenyl end-groups were more frequent at low polymerization temperatures. The formation of *cis*-2-butenyl and 4-butenyl terminated-chains appeared to be related to the regioirregular 2,1 insertion of a monomer unit since 4-butenyl end-groups were always detected when 2-butenyl terminals were present. The possible isomerization of 2-butenyl to 4-butenyl after polymerization was ruled out, and we postulated that the isomerization was produced by trace amounts of a zirconocene hydride complex present during polymerization.

The estimation of kinetic rate constants was performed using on-line measurements of the reaction rate and end-of-batch measurements of molecular weight distribution and percentage of unsaturated end-groups. Experimental data from the twelve runs carried out at different reaction conditions were used to estimate the Arrhenius form of the rate constants. Unlike other modeling works where the kinetic parameters were estimated by trial-and-error procedures,[13, 15] a systematic optimization strategy was used to solve the parameter estimation problem. The kinetic model produced good agreement with experimental polymerization rate curves. The estimated kinetic parameters suggested that the insertion of the first monomer unit is rate limiting relative to propagation. A theoretical Schultz-Flory distribution of molecular weights and constant M_W with M were predicted. The kinetic model yields comparatively poor estimates of molecular weights due to the ambiguous experimental trend of M_w with respect to M. Thus, the assumption of bimolecular β-hydride elimination as the main chain transfer

Table 6. Measured and Predicted Percentage of End-Group Assuming only the Formation of Vinylidene and Butenyl Unsaturations

	Experimental[(a)(b)]		Predicted	
Run	% Vinylidene	% Butenyl	% Vinylidene	% Butenyl
1	57.6	42.4	37.2	62.8
2	44.0	56.0	37.2	62.8
3	54.1	45.9	37.2	62.8
4	48.0	52.0	37.2	62.8
5	79.3	20.7	66.8	33.2
6	66.0	34.0	66.8	33.2
7	63.7	36.3	66.8	33.2
8	53.7	46.3	66.8	33.2
9	100.0	trace	81.1	18.9
10	86.8	13.2	81.1	18.9
11	79.2	20.8	81.1	18.9
12	82.6	17.4	81.1	18.9

[(a)]trace: signal close to the limit of detection. [(b)]Percentage of butenyl for run 9 was not included in the optimization of kinetic parameters.

Table 7. Regioirregular 2,1 Insertion of Propylene Units Predicted by the Kinetic Model

T (°C)	2,1 Insertion (mol %)
50	0.26
65	0.17
75	0.13

reaction must be reevaluated in future work. The model correctly predicted the decreasing percentage of butenyl-terminated chains relative to vinylidene-terminated chains with increasing temperature.

The developed kinetic model is restricted to catalyst systems that undergo a bimolecular chain transfer reaction as the main termination event. In the future, the kinetic model will be extended to different catalyst systems and polymerization conditions by including a monomolecular chain transfer reaction. Furthermore, the influence of the MAO/Zr ratio on reaction rate, molecular weight and microstructure of the final polymer chain will be studied and included in the kinetic model.

Acknowledgments

Funding for this work was provided in part by the General Electric Corporation and the University of Massachusetts. Central analytical facilities used in these studies were supported by the NSF-sponsored Materials Research Science and Engineering Center on Polymers at UMass Amherst (DMR-0213695).

Literature Cited

1. Sinclair, K. B. Future Trends in Polyolefins Materials. Macromol. Symp. 2001;173:237-61.
2. Wang, W.-J.; Yan, D.; Zhu, S.; Hamielec, A. E. Kinetics of Long Chain Branching in Continuous Solution Polymerization of Ethylene Using Constrained Geometry Metallocene. Macromolecules 1998;31(25):8677-83.
3. Moen, O. Models for Bench Scale Via Pilot to Commercial Scale. 2nd European Conference on the Reaction Engineering of Polyolefins. Lyon, France 2002.
4. Kaminsky, W. Highly Active Metallocene Catalysts for Olefin Polymerization. J. Chem. Soc. Dalton Trans. 1998:1413–18.
5. Chien, J. C. W.; Sugimoto, R. Kinetics and Stereochemical Control of Propylene Polymerization Initiated by Ethylene Bis(4,5,6,7-Tetrahydro-1-Indenyl) Zirconium Dichloride/Methyl Aluminoxane Catalyst. J. Polym. Sci. Part A: Polym. Chem. 1991;29:459-70.
6. Resconi, L.; Fait, A.; Piemontesi, F.; Colonnesi, M.; Rychlicki, H.; Zeigler, R. Effect of Monomer Concentration on Propene Polymerization with the rac-[Ethylenebis(1-indenyl)]zirconium Dichloride/Methylaluminoxane Catalyst. Macromolecules 1995;28(19):6667-76.
7. Carvill, A.; Zetta, L.; Zannoni, G.; Sacchi, M. C. *ansa*-Zirconocene-Catalyzed Solution Polymerization of Propene: Influence of Polymerization Conditions on the Unsaturated Chain-End Groups. Macromolecules 1998;31:3783-89.
8. Resconi, L.; Camurati, I.; Sudmeijer, O. Chain Transfer Reactions in Propylene Polymerization with Zirconocene Catalysts. Topics in Catalysis 1999;7:145-63.
9. Lin, S.; Tagge, C. D.; Waymouth, R. M.; Nele, M.; Collins, S.; Pinto, J. C. Kinetics of Propylene Polymerization Using Bis(2-phenylindenyl)zirconium Dichloride/Methylaluminoxane. J. Am. Chem. Soc. 2000;122(46):11275-85.
10. Kawahara, N.; Kojoh, S.; Matsuo, S.; Kaneko, H.; Matsugi, T.; Toda, Y.; Mizuno, A.; Kashiwa N. Study on Chain End Structures of Polypropylenes Prepared with Different Symmetrical Metallocene Catalysts. Polymer 2004;45:2883-88.
11. Wester, T. L.; Johnsen, H.; Kittilsen, P.; Rytter, E. The Effect of Temperature on the Polymerization of Propene with Dimethylsilylbis(1-indenyl)Zirconium Dichloride/Methylaluminoxane and Dimethylsilylbis(2-methyl-1-indenyl)Zirconium Dichloride/Methylaluminoxane. Modeling of Kinetics. Macromol. Chem. Phys. 1998;199:1989-2004.
12. Thorshaug, K.; Stovneng, J. A.; Rytter, E.; Ystenes, M. Termination, Isomerization, and Propagation Reactions during Ethene Polymerization Catalyzed by $Cp_2Zr\text{-}R^+$ and $Cp^*_2Zr\text{-}R^+$. An Experimental and Theoretical Investigation. Macromolecules 1998;31:7149-65.
13. Ochoteco, E.; Vecino, M.; Montes, M.; De la Cal, J. C. Kinetics and Properties in Metallocene Catalysed Propene Polymerisations. Chemical Engineering Science 2001;56:4169-79.
14. Fisher, D.; Mulhaupt, R. Reversible and Irreversible Deactivation of Propene Polymerization using Homogeneous Cp_2ZrCl_2/Methylaluminoxane Ziegler-Natta Catalysts. Journal of Organometallic Chemistry 1991;417:C7–C11.
15. Vela-Estrada, J. M.; Hamielec, A. E. Modelling of Ethylene Polymerization with Cp_2ZrCl_2/MAO Catalyst. Polymer 1994;35(4):808-18.
16. Huang, J.; Rempel, G. L. Kinetic Study of Propylene Polymerization using $Et(H_4Ind)_2ZrCl_2$/MAO. Ind. Eng. Chem. Res. 1997;36(4):1151-57.
17. Belelli, P. G.; Ferreira, M. L.; Lacunza, M. H.; Damiani, D. E.; Brandolin, A. Propylene Polymerization in a Semibatch Reactor. Analysis of Soluble Metallocene Catalyst Behavior Through Reactor Modeling. Polymer Engineering and Science 2001;41(12):2082-94.
18. Nele, M.; Collins, S. Two-State Models for Olefin Polymerization using Metallocene Catalysts. 1. Application to Fluxional Metallocene Catalyst Systems. Macromolecules 2000;33:7249-60.
19. Nele, M.; Mohammed, M.; Xin, S.; Collins, S. Two-State Models for Propylene Polymerization Using Metallocene Catalysts. 2. Application to *ansa*-Metallocene Catalyst Systems. Macromolecules 2001;34:3830-41.
20. Atiqullah, M.; Hammawa, H.; Hamid, H. Modeling the solubility of ethylene and propylene in a typical polymerization diluent: some selected situations. Eur. Polym. J. 1998;34(10):1511-20.
21. Mori, S.; Barth, H. G. Size Exclusion Chromatography. Berlin: Springer Laboratory; 1999.
22. Galli, P. The reactor granule technology: The ultimate expansion of polypropylene properties? J.M.S.-Pure Appl. Chem. 1999;A36(11): 1561-86.
23. Carvill, A.; Tritto, I.; Locatelli, P.; Sacchi, M. C. Polymer Microstructure as a Probe into Hydrogen Activation Effect in ansa-Zirconocene/Methylaluminoxane Catalyzed Propene Polymerizations. Macromolecules 1997;30(23):7056-62.
24. Kim, I.; Zhou, J. M.; Won, M. S. Kinetics of Propylene Polymerization Initiated by rac-$Me_2Si(1\text{-}C_5H_2\text{-}2\text{-}Me\text{-}4\text{-}Bu\text{-}t)(2)Zr(NMe_2)(2)$/MAO Catalyst. J. Polym. Sci. Part A: Polym. Chem. 1999;37(6):737-50.
25. Busico, V.; Cipullo, R. Effects of Regiochemical and Stereochemical Errors on the Course of Isotactic Propene Polyinsertion Promoted by Homogeneous Ziegler-Natta Catalysts. Macromolecules 1994;27:7538-43.
26. Resconi, L.; Piamontesi, F.; Camurati, I.; Sudmeijer, O.; Nifant'ev, I. E.; Ivchenko, P. V.; Kuz'mina, L. G. Highly Regiospecific Zirconocene Catalysts for the Isospecific Polymerization of Propene. J. Am. Chem. Soc. 1998;120:2308-21.
27. Resconi, L. On the Mechanisms of Growing-Chain-End Isomerization and Transfer Reactions in Propylene Polymerization with Isospecific, C_2-Symmetric Zirconocene Catalysts. Journal of Molecular Catalysis A: Chemical 1999;146:167-78.
28. Kawahara, N.; Kojoh, S.; Toda, Y.; Mizuno, A.; Kashiwa, N. The Detailed Analysis of the Vinylidene Structure of Metallocene-Catalyzed Polypropylene. Polymer 2004;45(2):355-57.
29. Schaverien, C. J.; Ernst, R.; Schut, P.; Dall'Occo, T. Ethylene Bis(2-indenyl) Zirconocenes: A New Class of Diastereomeric Metallocenes for the (co)Polymerization of alpha-olefins. Organometallics 2001; 20(16):3436-52.
30. Finlayson, B. A. Nonlinear Analysis in Chemical Engineering. New York: McGraw-Hill; 1980.
31. Liu, Z.; Somsook, E.; Landis, C. R. A ^{2}H-Labeling Scheme for Active-Site Counts in Metallocene-Catalyzed Alkene Polymerization. J. Am. Chem. Soc. 2001;123(12):2915-16.
32. Busico, V.; Cipullo, R.; Esposito, V. Stopped-Flow Polymerizations of Ethene and Propene in the Presence of the Catalyst System *rac*-$Me_2Si(2\text{-}methyl\text{-}4\text{-}phenyl\text{-}1\text{-}indenyl)(2)ZrCl_2$/Methylaluminoxane. Macromol. Rapid Commun. 1999;20(3):116-21.
33. Busico, V.; Cipullo, R. Microstructure of Polypropylene. Prog. Polym. Sci. 2001;26:443-533.
34. Ferreira, M. L. A Proposed Mechanism for Olefin Polymerization, 1 - C_{2v}, C_2 and C_s Zirconocene Catalysts. Macromolecular Theory and Simulations 2002;11(3):250-66.
35. Quicker, G.; Schumpe, A.; Deckwer, W. D. Gas-liquid interfacial-areas in a bubble column with suspended-solids. Chemical Engineering Science 1984;39(1):179-83.
36. Floyd, S.; Hutchinson, R. A.; Ray, W. H. Polymerization of Olefins Through Heterogeneous Catalysis-V. Gas-Liquid Mass Transfer Limitations in Liquid Slurry Reactors. Journal of Applied Polymer Science 1986;32(6):5451-79.

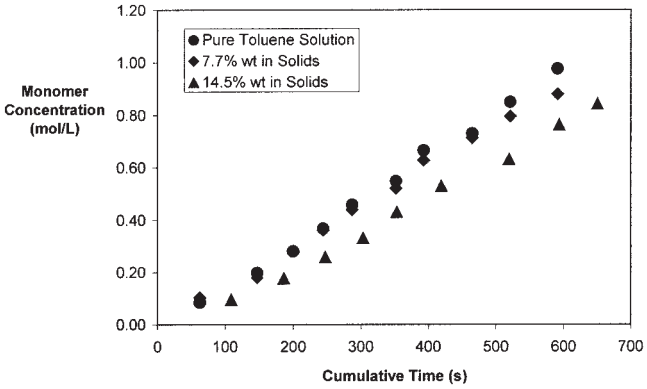

Figure A1. Cumulative time to reach equilibrium monomer concentration for three levels of polymer solids: (●) 0% wt, (◆) 7.7% wt, (▲) 14.5% wt.

Appendix

Mass-transfer limitation

Polymerization rate was measured by monitoring monomer consumption while keeping the pressure constant during the reaction. To have a constant propylene concentration in the liquid phase, the rate of mass transfer must be fast relative to the rate of reaction (the reaction must be kinetically controlled). A preliminary analysis to evaluate the rate of mass transfer of propylene was performed to ensure that the production of polymer does not influence the propylene concentration through mass transfer effects.[9]

To determine the effects of mass transfer in the semi-batch polymerization runs, a series of three experiments were performed measuring the absorption of propylene between equilibrium states: one in pure solvent (toluene) and two runs observing the effect of gas transport in a polymer-solvent mixture at different levels of solid content (7.7% wt and 14.5% wt). All runs were performed at 50°C and 1250 rpm of agitation with propylene partial pressures between 1.4 to 3.5 atm and using isotactic polypropylene powder as the solid. After thermal and pressure stabilization the system was forced to be at a higher pressure by injecting propylene, and the amount of time for the system to reach equilibrium was measured. The monomer concentration corresponding to the partial pressure was calculated by determining fugacities of monomer and solvent in both phases using the Peng-Robinson equation of state. Using the data presented in Figure A1, a mass transfer coefficient (k_La) for propylene in the liquid phase was calculated using Eq. A1.

Table A1. Mass-Transfer Coefficient for Propylene in Slurry with Toluene at 50°C

Solution	k_La (s^{-1})
Pure Toluene	2.11E−02
7.7% wt solids	1.81E−02
14.5% wt solids	1.54E−02

$$\frac{d[M]_{Liq}}{dt} = k_La([M]_{eq} - [M]_{Liq}) \tag{A1}$$

Average k_L results are presented in Table A1. Reductions in the mass transfer coefficient by the polymer were not dramatic up to 14.5% wt. However, other authors have reported a considerable reduction in k_La for polymer solid concentrations above 30% wt.[35] This criterion limited the reaction time in the experiments performed to avoid solid contents above 30% wt. With knowledge of the mass transfer coefficient, a simple quasi-steady-state material balance (Eq. A2) provided a prediction of the mass transfer resistance effect on the observed polymerization rate (R_{obs}) at 50°C.[36]

$$\frac{R_{obs}}{R_{ideal}} = \frac{k_La - R_{obs}[M]_{eq}}{k_La} \tag{A2}$$

where R_{ideal} is the "ideal" reaction rate in the absence of any mass transfer resistance. Based on this analysis, Table A2 shows that mass transfer resistance will always be present during the polymerization. Minimization of the mass transfer effect was achieved by using a high agitation speed and avoiding high solids content at the end of each batch.

Reproducibility test

Reproducibility in the measurement of polymerization rate and polymer properties was tested by performing two duplicate runs at 50°C and 1.5 atm. The absolute time average difference between both reaction rates was 6.2×10^{-3} mol/L min. An analysis of variance (ANOVA) statistical test was carried out for the measurements of weight average molecular weight (M_w) and percentage of butenyl end-group for the obtained polymer. Four measurements of M_w and three measurements of percentage of end-groups were performed for each run. The pooled standard deviation for M_w was 1182 g/mol and for the percentage of butenyl end-groups was 3.5%. The p-value of the ANOVA test for M_w was 7.4%, and for the percentage of butenyl was 55.7%.

Table A2. Evaluation of Mass-Transfer Effects on Experimental Runs at 50°C Using *rac*-Et(Ind)$_2$ZrCl$_2$/MAO

Pressure (atm)	Temperature (°C)	Solid Content (% wt)	k_L^*a[(a)] (s^{-1})	M_{eq} (mol/L)	Average R_{obs} (mol/L s)	R_{obs}/R_{ideal}[(b)]
1.5	50	12.2	1.62E−02	0.60	8.17E−04	0.916
2.5	50	11.0	1.67E−02	1.09	6.70E−02	0.939
3.2	50	14.6	1.53E−02	1.47	1.06E−01	0.921
3.8	50	13.4	1.58E−02	1.83	1.35E−01	0.922

[(a)]The value of k_La was calculated by linear interpolation of the values reported in Table 1 with respect of solid contents. [(b)]Value equal to 1 indicates no mass transfer resistance.

Manuscript received Jun. 22, 2005, and revision received Nov. 21, 2005.